ACS OMEGA

Open Access

http://pubs.acs.org/journal/acsodf

Article

Rational Design Problematics of Peptide Nucleic Acids as SARS-CoV-2 Inhibitors

Published as part of ACS Omega virtual special issue "3D Structures in Medicinal Chemistry and Chemical Biology".

Tatyana A. Grigoreva,* Svetlana V. Vorona, Daria S. Novikova, and Vyacheslav G. Tribulovich

Cite This: *ACS Omega* 2024, 9, 33000−33010

Read Online

ACCESS | Metrics & More | Article Recommendations

ABSTRACT: The use of viral protein inhibitors has shown to be insufficiently effective in the case of highly variable SARS-CoV-2. In this work, we examined the possibility of designing agents that bind to a highly conserved region of coronavirus (+)RNA. We demonstrated that while the design of antisense RNAs is based on the complementary interaction of nitrogenous bases, it is possible to use semirigid docking methods in the case of unnatural peptide nucleic acids. The transition from N-(2-aminoethyl)glycine chain to a more conformationally rigid piperidine-containing backbone allowed us to significantly increase the affinity of structures to the target RNA.

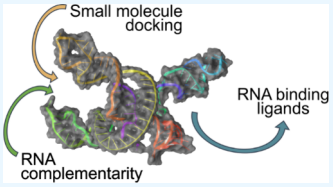

1. INTRODUCTION

Covid19 was not the first coronavirus pandemic and clearly showed that since the epidemics of SARS-CoV (Severe Acute Respiratory Syndrome−related CoronaVirus, 2002−2004 outbreak) and MERS-CoV (Middle East Respiratory Syndrome−related CoronaVirus 2012 outbreak), no significant achievements in the fight with similar diseases were made. Despite the efforts of both clinicians and drug developers, in fact, the effective therapy for severe respiratory syndromes is still missing.

SARS-CoV-2 (Severe Acute Respiratory Syndrome−related CoronaVirus 2) is an enveloped single-stranded (+)RNA virus, which means that the synthesis of viral proteins can occur on ribosomes of a human cell directly on (+) genomic RNA of the virus without additional stages. When entering the cell, the virus expresses its own RNA-dependent RNA polymerase and a number of other enzymes that ensure replication, processing and transcription of RNA, including spike (S), envelope (E), membrane (M), and nucleocapsid (N) structural proteins, 16 nonstructural proteins (NSPs) that make up the replicase complex, and 9 accessory proteins (ORFs).[1−4]

Figure 1[5] demonstrates that all significant proteins encoded by the virus have been sufficiently well studied and, accordingly, can be used for rational drug design. At the moment, there are several approaches to combating SARS-CoV-2 in the body. In addition to the use of vaccines, approaches based on preventing the interaction of the virus with the cell and disrupting intracellular processes are possible.

In the first case, it is proposed to affect SARS-CoV-2 spike protein: either through immunization with appropriate vaccines, or by inhibiting the interaction of the S protein receptor-binding domain with the human angiotensin-converting enzyme 2 (ACE2) receptor.[6−11] Among disadvantages of such agents is the high probability of mutations in the S protein,[7,12] typical for RNA viruses, as well as the possibility of using alternative receptors by the virus.

The central enzyme of transcription and replication is the RNA-dependent RNA polymerase (RdRp). It synthesizes all viral RNA and is a proven target for antiviral drugs, being of great interest to researchers. It is the functioning of this enzyme that can be affected by nucleoside analogues, such as remdesivir and molnupiravir, which, being integrated into the growing RNA chain, induce immediate pausing of RNA synthesis.[3,13] There are many new developments among nucleoside analogues,[14] but antiviral drugs originally proposed against other viruses, such as favipiravir[15] and ribavirin,[16] also have an effect against SARS-CoV-2.

While nucleoside inhibitors bind to the RdRp protein at the enzyme active site, nonnucleoside inhibitors bind to the RdRp protein at allosteric sites.[14] In the case of SARS-CoV-2, the RdRp inhibitor of influenza A virus pimodivir[17] and hepacivirus C NS5B polymerase inhibitors[14] were considered, although without much success.

The N protein of SARS-CoV is the most abundantly expressed of the structural proteins during infection.[18] Like the S protein, it induces a strong antibody response in hosts.[4] The

Received: April 27, 2024
Revised: June 24, 2024
Accepted: July 5, 2024
Published: July 16, 2024

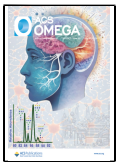

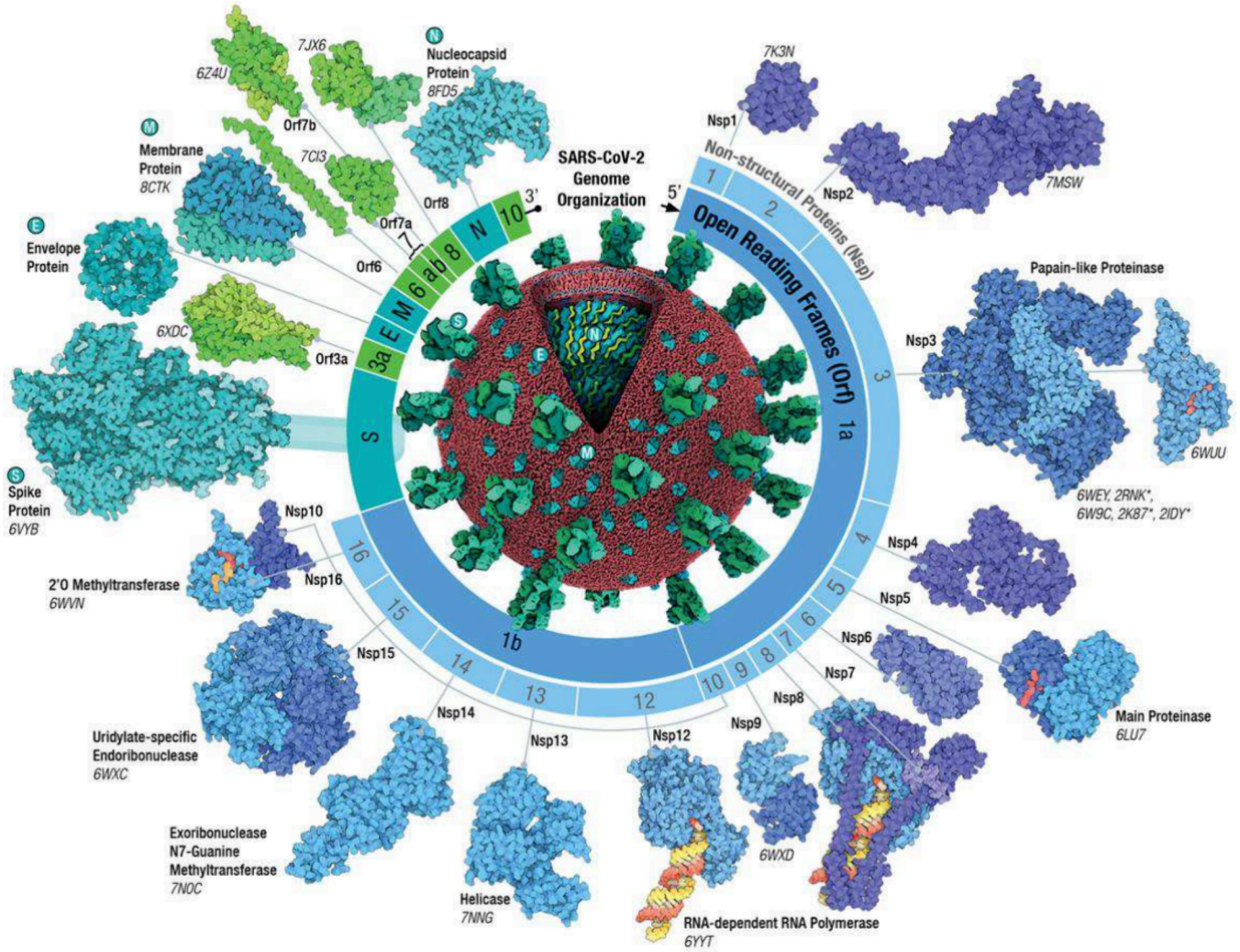

Figure 1. SARS-CoV-2 Genome and Proteins. Reprinted with permission from ref 5. Copyright 2023 PLOS.

fundamental function of the N protein is to package the viral genome RNA into a long helical ribonucleocapsid complex, and also it participates in the assembly of the virion through its interactions with the viral genome and membrane protein M.[19] Based on the conservation of the N protein of coronaviruses in evolution and its key role in viral replication, it is considered as a promising target for drug discovery.[4] In particular, the authors[20] proposed an interesting approach based on the N protein dimerization by a small molecule compound, 5-benzyloxygramine.

Processing of polyproteins synthesized on the SARS-CoV-2 single-stranded RNA template is carried out by the main protease (M^{pro}), also known as the 3C-like protease ($3CL^{pro}$). Moreover, M^{pro} active sites are highly conserved among all coronaviruses and are well studied, which allows one to propose rationally designed inhibitors.[21−23] An extensive number of studies have been devoted to the development of inhibitors of this protein, which is facilitated by the presence of the structures cocrystallized with inhibitors. Thus, the authors[24,25] started from the structures of crystallized inhibitors, proposing new inhibitory peptidomimetics. Modifications of the known hepatitis C virus protease inhibitor boceprevir allowed obtaining orally bioavailable compounds,[26,27] and it was shown that they may be less sensitive to several mutations that cause resistance in the natural SARS-CoV-2 population.[26] As the availability of computer modeling methods increases, researchers are gradually supplementing them with modern technologies of artificial intelligence and deep learning;[23,28,29] however, approaches based on screening of chemical libraries[30] are also on top of their relevancy.

Despite serious efforts aimed at developing protein inhibitors of the SARS-CoV-2 virus, the effective therapy remains unavailable, which may be primarily due to the high degree of variability of the virus and its rapid adaptation to drugs. In such a situation, a solution may be the use of antisense therapy, which has already shown its effectiveness in the clinical treatment of a number of diseases.[31]

RNA therapeutics, including siRNAs, antisense oligonucleotides (ASO), and other oligonucleotides, possesses a great potential in the selective treatment of various human diseases, starting from cancer to COVID and Parkinson's disease.[32] It is assumed that a synthetic oligonucleotide will interact with the target RNA through Watson−Crick base pairing; as a result of the formation of such a complex, either the destruction of the target or prevention of its reading out should occur.

One of the major advantages of ASOs is the possibility to target any conserved sequence as the positive or negative RNA strand. This allows SARS-CoV-2 RNA targeting at any step of the viral life cycle.[33] The first such agent was proposed in 2004[34] against the closely related SARS-CoV and demon-

https://doi.org/10.1021/acsomega.4c04023
ACS Omega 2024, 9, 33000−33010

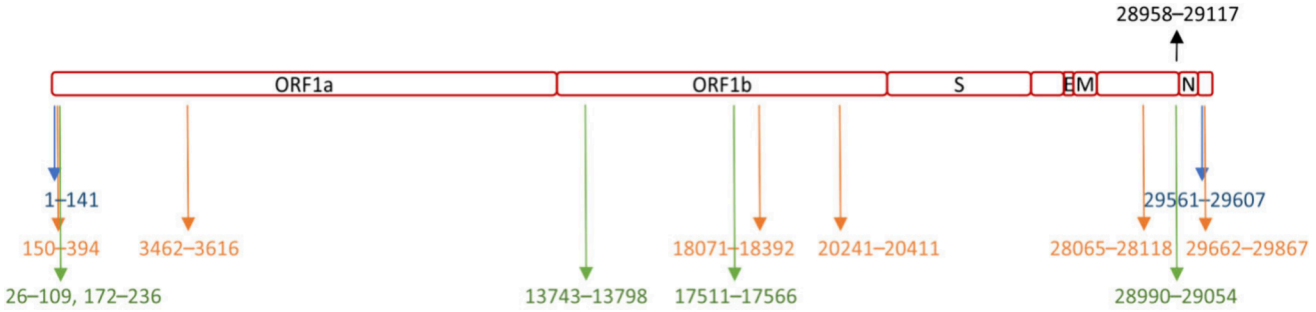

Figure 2. Potential sites for the interaction with ASOs (blue[35]) and small molecule ligands (orange[36]), as well as fragments highly conserved among SARS and MERS (green[39]). The region considered in this work is shown in black.

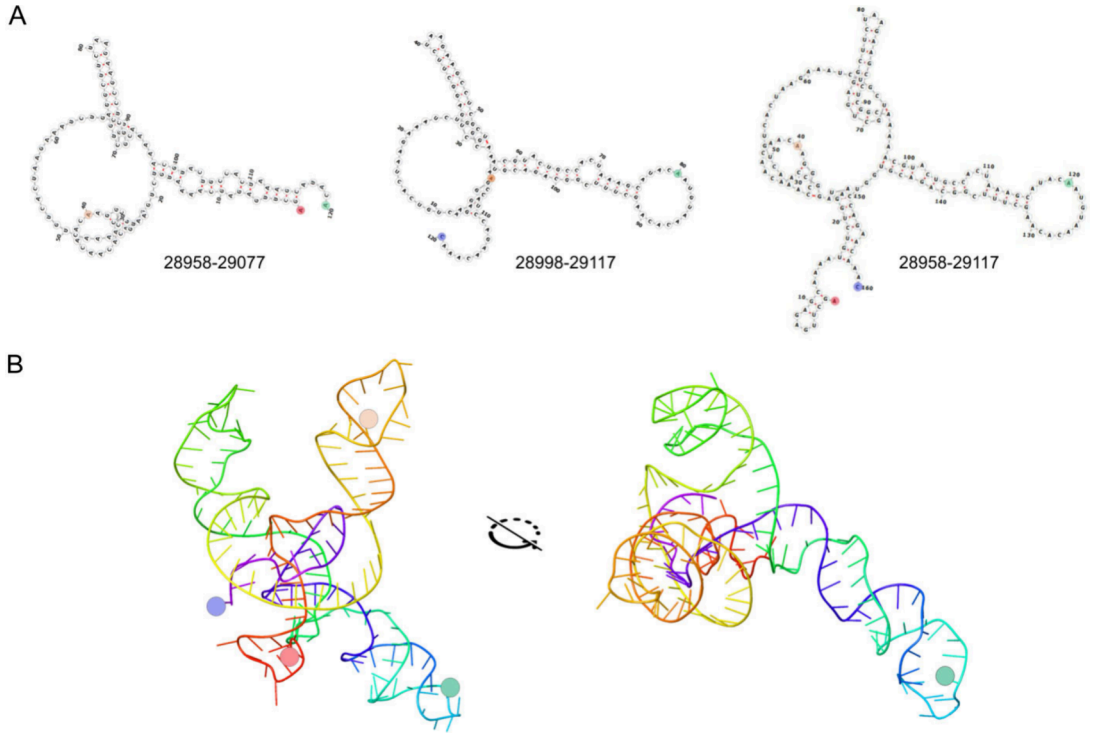

Figure 3. Spatial structure of the considered RNA region. (A) Generated two-dimensional structures of fragments 28958–29077, 28998–29117, and 28958–29117. (B) Three-dimensional structure of the fragment 28958–29117. Colors indicate adenines 28958 (red), 28998 (yellow), 29077 (green), and cytosine 29117 (blue).

strated high antiviral activity in vitro. Currently, a number of approaches to the development of anti-SARS ASOs[35,36] have been proposed, but nevertheless, not any highly effective variants have been developed so far. Moreover, despite extensive research on COVID-19, there is currently no effective treatment available for clinical use at all.[4]

In this work, we propose a new perspective on the use of modified oligonucleotides and explain a relatively low effectiveness of such compounds *in vivo* compared with oligonucleotides of a classical structure.

2. RESULTS AND DISCUSSION

2.1. Site Selection. In general, it is possible to create ASO that selectively binds to any base sequence and prevents reading out from the corresponding region of RNA, but certain regions may be considered preferential. The emphasis is on finding highly conserved fragments, binding to which allows one to expect a long-term effect, and which can be used for several related viruses.[35−37] In the case of coronaviruses, full-length positive-sense genomic RNA is used as a template to produce both full-length negative-sense copies for genome replication and subgenomic negative-sense RNAs to produce subgenomic mRNAs.[38] Accordingly, we believed it rational to consider regions of the virus genome near the 3′-end, because this region is read by RNA-dependent RNA polymerase many times. Since it was shown[39] that there is a number of highly conserved regions in the 3′-end region of coronavirus RNA, the impact on which should have an effect on various subspecies of coronavirus, we focused on the fragment 28958−29117, which includes one of such conserved regions (28990−29054, Figure 2).

Since this region allows the generation of a huge number of complementary oligonucleotides, we considered it appropriate to focus on spatially accessible RNA fragments, loops and hairpins. To date, several groups have simultaneously examined the 3′-end region of coronavirus RNA using different combinations of methods as reflected in the RNA-Puzzles challenge.[40] In our work, the spatial structure of fragments of

https://doi.org/10.1021/acsomega.4c04023
ACS Omega 2024, 9, 33000−33010

120 nucleotides long, as well as a full-length structure including 160 bases was generated *de novo* (Figure 3A). At the first step, the secondary structure was generated from the base sequence in dot-bracket format using RNAfold Web Service; then 3D structures were formed on its basis using RNAComposer server.[41−43] Comparison of the resulting structures showed a high degree of agreement, which allowed us to use the full-size fragment in further work. The stability of the resulting RNA configuration was confirmed by molecular dynamics data. The RMSD values of the structure fluctuated within 2 Å after relaxation. In the 3D structure of RNA, three hairpins (orange, green and blue), as well as small (red) and large (yellow) loops can be distinguished (Figure 3B). Each of these five elements was used as a site for docking because of its spatial accessibility.

2.2. PNA Design. It is believed that any RNA repeat longer than 13 bases can be found only once in the human genome;[44] therefore, this number of bases can be considered as a lower limit when designing antisense oligonucleotides complementary to the target. The upper limit is determined by the applied aspects, such as the complexity to synthesize a long chain and the problems of its bioavailability. In a selected region of RNA, a whole package of potential targets with a length of about 15 bases, typical for synthetic antisense oligonucleotides, can be used, and to narrow the range of considered structures, we relied on the spatial accessibility of RNA structural elements. As a result, sequences complementary to five selected regions were considered: three hairpins and two loops, in accordance with Figure 3B, a total of 20 sequences.

Varying the chemical structure of the oligonucleotide backbone can enhance potency, pharmacokinetics, and reduce toxicity.[33] The use of modified nucleic acids can significantly improve pharmacological properties, since such structures are not recognized by cellular systems, which makes them significantly more stable and less immunogenic.[45] A prominent example of an antisense therapy is Nusinersen (trade name Spinraza) for the treatment of spinal muscular atrophy.[46]

Peptide nucleic acids (PNAs) are promising drugs for the so-called “reversible gene modification”. Their main advantage is their resistance to degradation by proteases and nucleases, which determines their stability in biological environment.[47]

Along with the classical PNA backbone formed by an N-(2-aminoethyl)glycine chain, we also considered PNAs based on a piperidine scaffold, which form conformationally constrained structures (Figure 4).

The entire completed library of structures was subjected to primary processing. The structures of this size were found to be too large to use the LigPrep tool and were subjected to the conformational search procedure in MacroModel.[48] As a result, absolutely all structures, regardless of the sequence of bases and even the backbone collapsed into compact globules, which excludes the possibility of meaningful docking.

Since attempts to minimize extended PNAs invariably led to the folding of PNAs into compact globules, to test the methods we included PNAs with a length of 4−6 nucleotides, which are successfully processed by computational tools, in the spectrum of considered structures.

Differences in the behavior of PNA depending on the scaffold used appeared already at the stage of structure minimization, and the ratio of purine and pyrimidine bases in the molecule did not affect the observed trends. While classical PNAs, regardless of the method of generating conformations, showed a tendency to fold into globule-like structures, in the case of piperidine derivatives, the presence of a structured backbone contributed to the linearization of the structures (Figure 5).

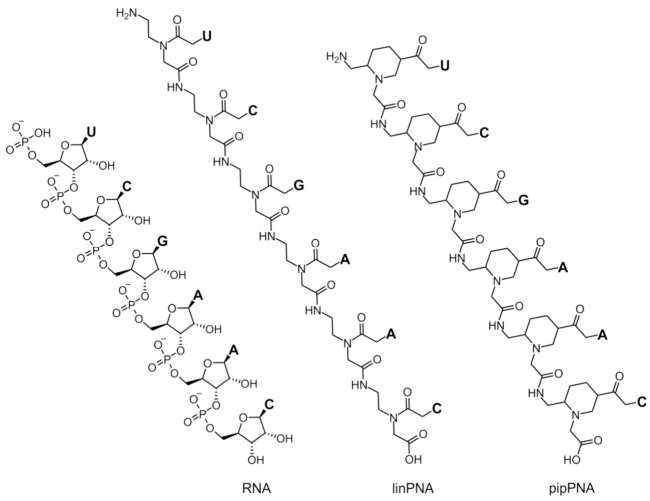

Figure 4. Structures of considered RNA and PNA as exemplified by the sequence UCGAAC.

Accordingly, one can expect that PNAs with different backbones will bind to RNA differently even if the nitrogenous bases in the structure are the same.

2.3. Hit Identification. It has to be noted that despite the growing interest in NA-targeting agents, we did not find an effective tool that predicts complementary interactions between RNA and backbone-altered nucleosides, since such programs only work with RNA and DNA (for example, RNAcofold from ViennaRNA web serveces[41] or HNADOCK server[49]). In addition, since large ligands cannot be modeled under semirigid docking mode, we used protein−protein docking implemented in Schrodinger Suite 2020−4. This approach also turned out to be inapplicable for PNA as one of the interaction participants; moreover, when modeling the interaction of two RNAs, the resulting spatial conglomerate turned out to be significantly different from the expected one (Figure 6).

Having received these results, we moved on to a detailed study of the interactions of short PNAs with the target using the method of flexible molecular docking implemented in the Glide program.[50] At the first step, we considered the interaction of a model structure of 4 modified bases with the most protruding region of the hairpin, where 3 nitrogenous bases U273, A275 and G276 are easily accessible for complementary interactions, while G274 forms intramolecular bonds (Figure 7A). Simulations of this interaction showed the formation of numerous hydrogen bonds (magenta) and Pi-Pi stacking (green), but the binding mode does not correspond to Watson−Crick base pairing (Figure 7B). Similar results were obtained with other PNAs in different regions of RNA.

Analysis of the cellular processes underlying the regulation of RNA reading out by other short RNAs allowed us to look at the creation of PNA from a new angle. The fact is that under native conditions, regulatory RNA bind target mRNA to prevent protein production by incorporating into the multi-component ribonucleoprotein complex RISC (RNA-induced silencing complex), which ensures the binding of RNA molecules to each other, while small RNA functions as a guide to silence target RNAs.[51,52] Accordingly, the selection of complementary bases makes sense only for the creation of

https://doi.org/10.1021/acsomega.4c04023
ACS Omega 2024, 9, 33000−33010

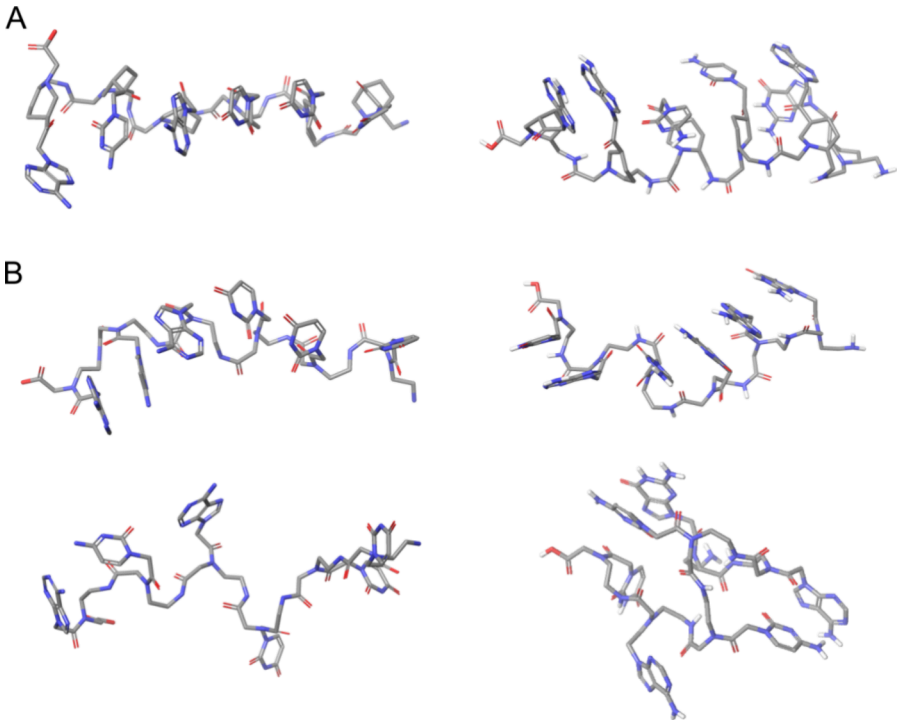

Figure 5. Folding of pipPNA (A) and linPNA (B) oligonucleotides formed from nitrogenous bases of the sequence UUUACA (left panel) and GACCAA (right panel).

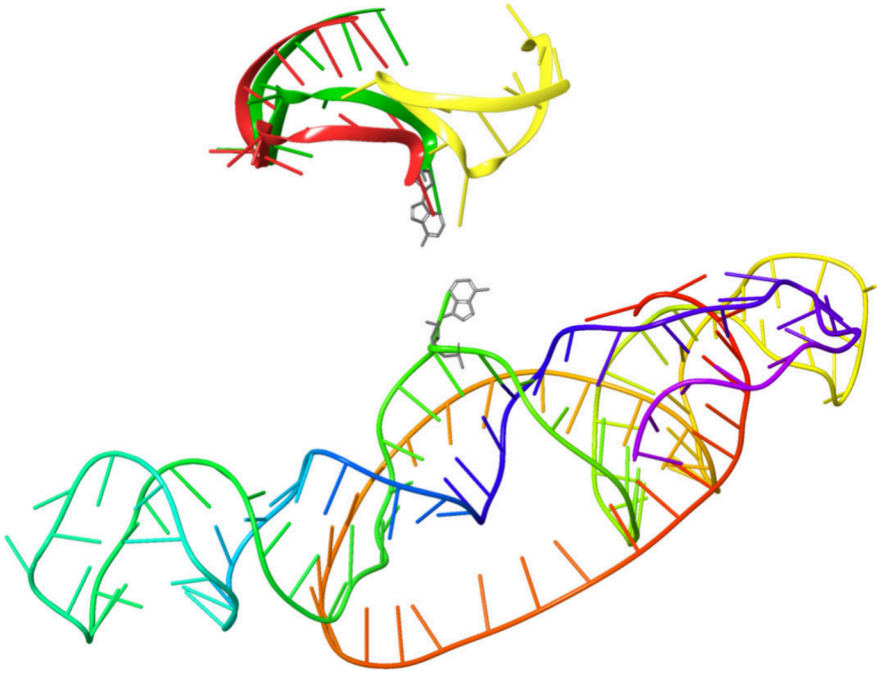

Figure 6. Result of modeling the interaction of two RNA molecules in protein−protein docking mode. The target is shown as thick tubes, and three AGCUUGAGAGCA molecules are shown as red, yellow, and green cartoons.

synthetic small RNAs, for which binding to other RISC components is possible, but not for structures with a different backbone, since in this case the assembly of the complex will not occur.

In the case of PNA, taking into account the specifics of RISC, it seems rational to shift toward classical docking with the search for small molecule ligands, considering the spatial structure of RNA similar to the three-dimensional structure of a protein. This approach echoes the idea reflected in,[36] where the authors used 3D modeling for the identification of druggable pockets for small molecule compounds. Since in this case there is no task to look for complementary interactions, we screened the entire PNA library for each of the five selected regions (Figure 8A). Additionally, we searched for sites using the SiteMap tool from Schrodinger Suite 2020−4,[53] (Figure 8B). Interestingly, although SiteMap does not see

https://doi.org/10.1021/acsomega.4c04023
ACS Omega 2024, 9, 33000−33010

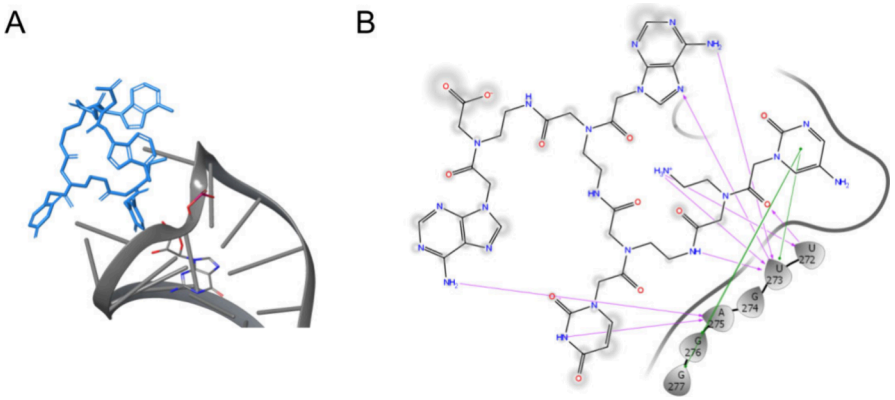

Figure 7. Interaction of CUAA PNA with the fragment ^{273}UGAG^{276}. 3D-view, PNA in blue thick tubes, G274 in thin tubes (A). Ligand interaction diagram, H-bonds are shown in magenta, Pi-Pi stacking is shown in green (B).

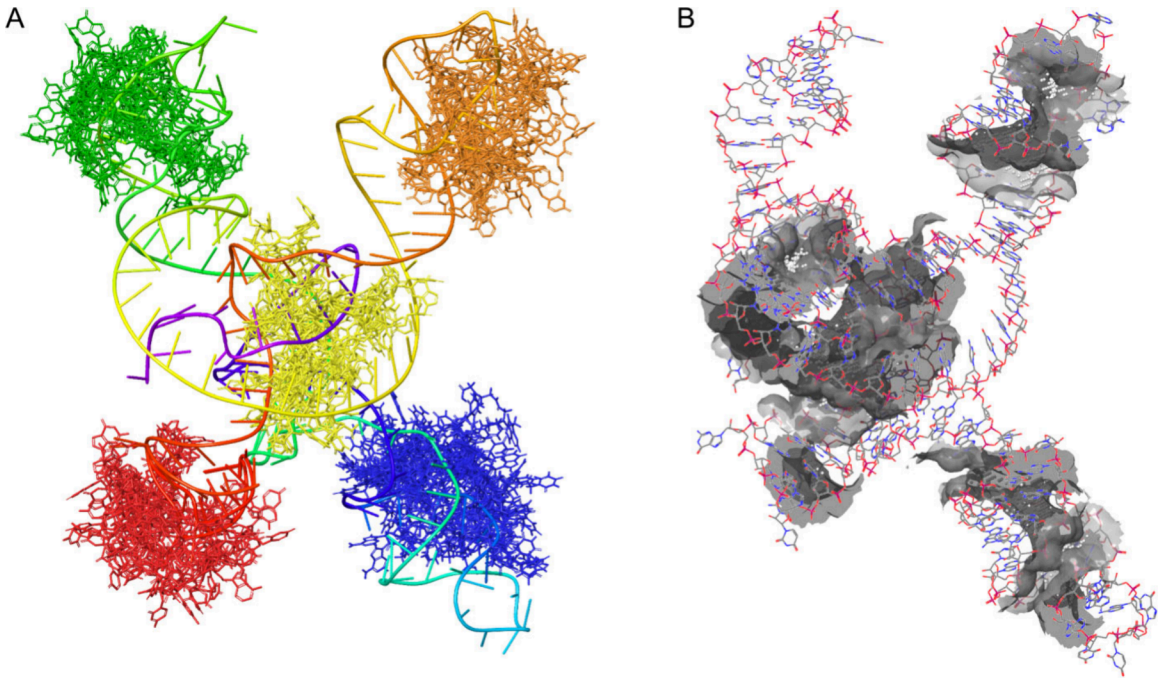

Figure 8. Sites of PNA interaction with target RNA. Result of docking into 5 selected regions corresponding to hairpins and loops (A), binding sites predicted by SiteMap (B).

potential binding sites on the green loop, the energetics of PNA interaction with the green and orange loops are at the same level (Table 1).

It should be noted that the complementarity principle actually turned out to be insufficiently informative in the case of the considered structures: the sequences showed an affinity to complementary RNA fragments, comparable to the affinity for other fragments. For example, pip3 bound weaker to the corresponding hairpin than to the other three regions. Nevertheless, a number of structures actually "fit" their fragments, for example, pip12, 15, 18 matched to the green hairpin or pip8, 9, 10 to the yellow loop. At the same time, several classical PNAs failed to bind their expected targets at all, such as lin3 to the orange hairpin or lin12, 13, 16 to the green hairpin.

In general, both linPNA and pipPNA bind most energetically to the yellow loop, which may be due to the larger contact surface in this region of RNA due to spatial features. In this site, as in the others, pipPNAs consistently show the best results, indicating the presence of not only a stabilizing, but also a binding role for the piperidine fragments of the backbone. Four pips (pip3, pip6, pip10, and pip21) show good results within 4 sites at once, while among linPNAs only lin14 shows Docking Score ≤ -11 within three sites, and lin17 and lin8 within two. While some linPNAs did not bind to RNA at all, no such data were found among pipPNAs, highlighting the role of the piperidine scaffold in the interaction.

Interesting results were obtained in the case of pip6 and pip10 when docked into the green loop: the scores were −64.5 and −65.6 kcal/mol, respectively, despite the fact that SiteMap does not consider this fragment significant. The binding poses of pip6, pip10, and pip18 (Docking Score = −14.9 kcal/mol) are shown in Figure 9. It can be seen that pip6, pip10 wind around the loop from the outside, while pip18 binds similar to intercalators, fitting between two strands of ribonucleic acid. It can be expected that such an interaction will effectively prevent the reading of the RNA region by both the RNA-dependent RNA polymerase and the ribosomal complex.

https://doi.org/10.1021/acsomega.4c04023
ACS Omega 2024, 9, 33000−33010

Table 1. Results of Docking of Modified Oligonucleotides into Five Target RNA Sites[a]

No.	Sequence	Scaffold	Docking Score, kcal/mol				
			Small loop	Hairpin	Large loop	Hairpin	Hairpin
1	GUUGUU	AminoAcid	–9.0	–9.0	–9.9	–7.1	–8.0
		Pip	–10.5	–12.4	12.3	–10.3	–10.9
2	UCGAAC	AminoAcid	–9.5	–9.4	–12.8	–8.6	–9.5
		Pip	–10.3	–9.6	–12.6	–9.1	–8.9
3	UCUCGU	AminoAcid	–10.1	-	–9.8	–7.5	–8.7
		Pip	–9.3	–11.2	–12.7	–11.9	–11.4
4	UUUACA	AminoAcid	–7.7	–7.9	–11.5	–6.3	–8.6
		Pip	–11.7	–12.3	–10.7	–10.9	–11.6
5	GACCAU	AminoAcid	–9.7	–7.6	–11.2	–8.4	–9.7
		Pip	–10.5	–12.8	–13.2	–10.3	–12.0
6	AGGUCU	AminoAcid	–9.3	–10.9	–11.6	–10.0	–8.2
		Pip	–12.6	–9.8	–11.4	–64.5	–11.9
7	UGUUUG	AminoAcid	–9.9	–9.0	–11.7	–9.4	–10.7
		Pip	–13.4	–11.6	–12.7	–9.9	–11.4
8	CAAACU	AminoAcid	–9.9	–7.2	–11.7	–10.6	–11.8
		Pip	–12.9	–11.4	–14.8	–10.2	–10.5
9	GUCACU	AminoAcid	–8.3	–7.2	–10.7	–8.5	–8.2
		Pip	–8.4	–8.6	–11.3	–10.8	–8.6
10	UUCUUU	AminoAcid	–9.6	–9.1	–11.7	–8.9	–10.7
		Pip	–13.4	–12.6	–11.4	–65.6	–9.5
11	AGACGA	AminoAcid	-	-	-	-	-
		Pip	–10.7	–9.8	–14.7	–8.6	–10.1
12	UUGCAU	AminoAcid	-	–5.7	-	-	–1.1
		Pip	–10.3	–9.2	–10.8	–12.3	–8.7
13	GACGGU	AminoAcid	-	-	-	-	-
		Pip	–8.4	–10.1	–13.2	–12.0	–12.5
14	UGUUAC	AminoAcid	–10.9	–8.7	–10.7	–11.2	–11.7
		Pip	–10.5	–12.8	–11.5	–9.0	–8.2
15	AUUGUG	AminoAcid	–10.1	–10.0	–13.1	–9.6	–9.7
		Pip	–10.9	–9.1	–10.9	–12.6	–8.8
16	GAAAGC	AminoAcid	-	-	-	-	-
		Pip	–13.3	–9.7	–9.4	–11.0	–8.6
17	CGUCUG	AminoAcid	–12.4	–9.4	–10.3	–9.5	–8.9
		Pip	–11.0	–12.0	–10.3	–9.3	–10.5
18	GGUGAU	AminoAcid	–10.9	–8.8	–13.1	–8.8	–7.9
		Pip	–11.8	–13.6	–10.8	–14.9	–8.5
19	UUCGUA	AminoAcid	–7.5	-	–8.8	–3.9	–6.2
		Pip	–10.2	–9.9	–12.0	–9.8	–10.2
20	ACGACU	AminoAcid	–6.7	–6.2	–8.4	–5.7	–7.4
		Pip	–9.4	–10.6	–11.2	–11.2	–9.4
21	CCGAAG	AminoAcid	–7.9	–9.4	–9.8	–9.6	–8.9
		Pip	–11.1	–10.3	–14.4	–13.2	–11.8
22	UCUUCG	AminoAcid	–9.3	–8.8	–7.5	–9.1	–10.9
		Pip	–11.0	–9.7	–13.6	–10.1	–9.7
23	GAGCCG	AminoAcid	–8.9	–8.9	–11.1	–9.6	–8.8
		Pip	–14.0	–10.6	–13.8	–11.1	–9.7

[a]The highlight color of the sequence corresponds to the complementary RNA fragment (Figure 8).

https://doi.org/10.1021/acsomega.4c04023
ACS Omega 2024, 9, 33000−33010

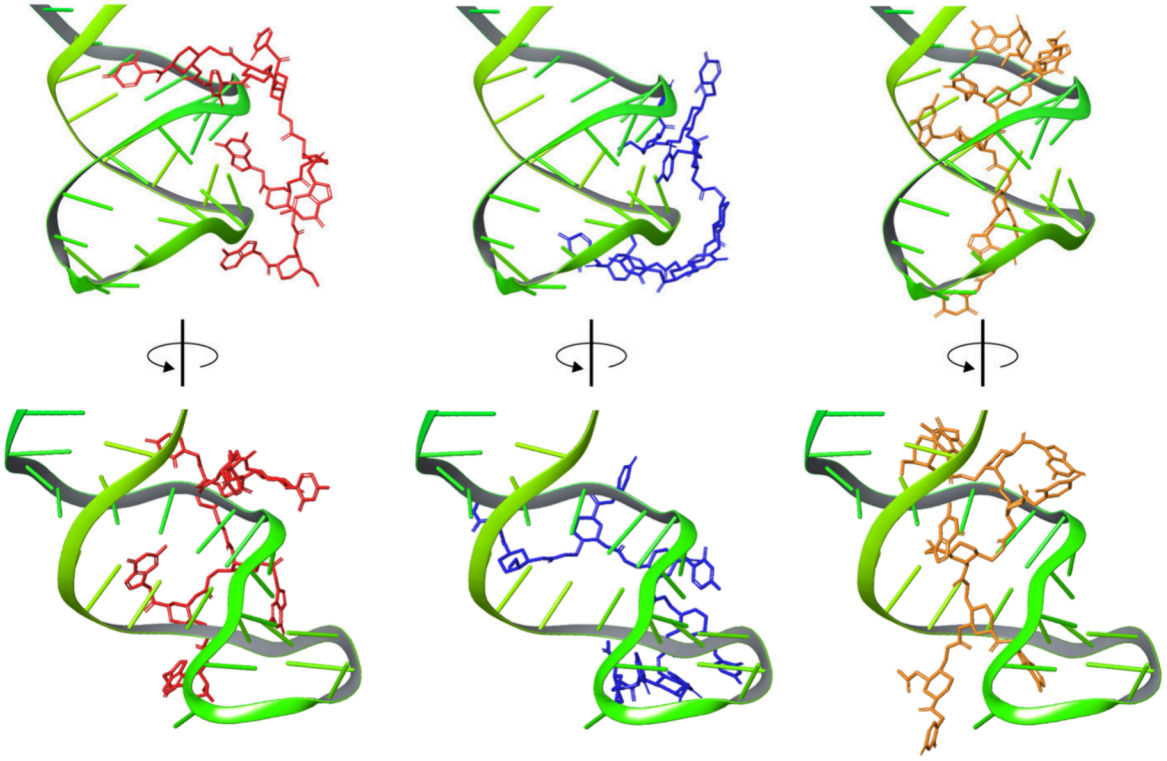

Figure 9. Binding of pip6 (red), pip10 (blue), and pip18 (yellow) to the green hairpin of RNA.

3. CONCLUSIONS

Coronaviruses have proven to be difficult targets for drug development as evidenced by the lack of effective therapy despite years of research. Due to the high rate of adaptation of the viruses to various protein-targeting agents, the use of ASO appears to be a promising approach in this field. The complementarity principle can be effectively used to create short antisense RNAs; however, such molecules have a number of disadvantages, including low solubility and a high rate of destruction by cellular enzymes. At the same time, varying the backbone, in particular the use of PNA, allows one to overcome these disadvantages.

In this work, we showed that PNAs can effectively interact with target RNA; however, for their design, it makes sense to deviate from the principle of selecting paired oligonucleotides. Screening of small molecule ligands based on docking structures into binding sites on the surface of bulk RNA fragments will allow the identification of optimal structures with high affinity to the target. If the target site is chosen correctly, it will be possible to achieve high-quality suppression of virus replication by preventing the interaction of RNA-dependent RNA polymerases or ribosomal complexes with the target RNA.

4. MATERIALS AND METHODS

4.1. RNA Structure Preparation. The secondary structure of single stranded RNA in the dot-bracket format was generated using RNAfold from the set of ViennaRNA Web Services (http://rna.tbi.univie.ac.at/cgi-bin/RNAWebSuite/RNAfold.cgi).[41]

Nucleic acid tertiary structure was generated by RNAComposer, a fully automated RNA structure modeling server (https://rnacomposer.cs.put.poznan.pl/)[42,43] using the RNA sequence and secondary structure in the dot-bracket format. The resulting 3D models in the .pdb format were integrated into the Maestro program, Schrödinger, LLC, New York, NY.

4.2. PNA Generation. PNAs were selected based on the complementarity principle using the publicly available form http://molbiol.ru/scripts/01_12.html. Small molecule structures with modified backbones were drawn in ChemBioDraw Ultra 14.0 (PerkinElmer). The generation of 3D structures of small molecules was performed using one of the tools implemented in Schrödinger Suite 2020−4 (Schrödinger, LLC, New York, NY).

In the case of full-length ASO, the method of conformational search implemented in MacroModel force field-based molecular modeling tool[38] that uses brief MD simulations followed by minimization and normal-mode search steps was used. For structures consisting of 4−6 bases, the LigPrep tool and MacroModel minimization were used using OPLS3e force field with the generation of tautomers and stereoisomers.[54−56]

Molecular dynamics was simulated using the Desmond module[57] of the Schrodinger Suite 2020−4 (Schrödinger, LLC, New York, NY). The RNA model was placed in an orthorhombic box with a buffer zone of 40 Å from the surface. The simulation area was filled with a model solvent simulating saline (water, SPC model). The charge of the system was neutralized by adding additional sodium ions. The molecular system was preminimized and equilibrated. Simulation parameters: time 50 ns; NPT environment; temperature 298 K; and registration step 50 ps. The OPLS3e force field was used.

4.3. Ligand-Protein Docking. To parametrize the binding of modified oligonucleotides to target RNA, we used the methods of flexible molecular docking implemented in the Glide program[50] and protein−protein docking program PIPER.[58]

https://doi.org/10.1021/acsomega.4c04023
ACS Omega 2024, 9, 33000−33010

The grid for molecular docking was generated in such a way that with a size of 34 Å the entire surface of the RNA molecule considered was utilized, at the same time we got 5 regions. Up to 10 poses were generated for each structure. The optimality of posing was determined based on the GlideScore and Emodel indicators, as well as on the clustering ability of docking solutions. The ligand's Docking Score, which was automatically calculated in the Glide program by adding the state penalty for a given protonation or tautomeric state of a ligand to the empirical scoring function GlideScore, was used to quantitatively compare the interaction of oligonucleotides to target RNA.

In the case of protein−protein docking, no restraints were imposed; up to 30 poses were considered with 70,000 ligand rotations to probe.

AUTHOR INFORMATION

Corresponding Author

Tatyana A. Grigoreva − *Laboratory of Molecular Pharmacology, St. Petersburg State Institute of Technology (Technical University), St. Petersburg 190013, Russia;* orcid.org/0000-0003-1271-0328; Email: rozentatiana@gmail.com

Authors

Svetlana V. Vorona − *Laboratory of Molecular Pharmacology, St. Petersburg State Institute of Technology (Technical University), St. Petersburg 190013, Russia;* orcid.org/0000-0002-7321-5702

Daria S. Novikova − *Laboratory of Molecular Pharmacology, St. Petersburg State Institute of Technology (Technical University), St. Petersburg 190013, Russia;* orcid.org/0000-0002-5310-4570

Vyacheslav G. Tribulovich − *Laboratory of Molecular Pharmacology, St. Petersburg State Institute of Technology (Technical University), St. Petersburg 190013, Russia;* orcid.org/0000-0001-7723-4962

Complete contact information is available at: https://pubs.acs.org/10.1021/acsomega.4c04023

Notes

The authors declare no competing financial interest.

ACKNOWLEDGMENTS

The work was supported by the Russian Science Foundation (project no. 22-73-00328).

ABBREVIATIONS

PDB, Protein Data Bank; PNA, Peptide nucleic acid; ASO, Antisense oligonucleotides; SARS-CoV, severe acute respiratory syndrome-related coronavirus; MERS-CoV, Middle East respiratory syndrome-related coronavirus; NSP, nonstructural protein; ORF, open reading frame; M^{pro}, main protease; $3CL^{pro}$, 3C-like protease; ACE2, angiotensin-converting enzyme 2; RdRp, RNA-dependent RNA polymerase

REFERENCES

(1) Wu, F.; Zhao, S.; Yu, B.; Chen, Y. M.; Wang, W.; Song, Z. G.; Hu, Y.; Tao, Z. W.; Tian, J. H.; Pei, Y. Y.; et al. A new coronavirus associated with human respiratory disease in China. *Nature* **2020**, *579* (7798), 265−269.

(2) Lu, R.; Zhao, X.; Li, J.; Niu, P.; Yang, B.; Wu, H.; Wang, W.; Song, H.; Huang, B.; Zhu, N.; Bi, Y.; Ma, X.; Zhan, F.; Wang, L.; Hu, T.; Zhou, H.; Hu, Z.; Zhou, W.; Zhao, L.; Chen, J.; Meng, Y.; Wang, J.; Lin, Y.; Yuan, J.; Xie, Z.; Ma, J.; Liu, W. J.; Wang, D.; Xu, W.; Holmes, E. C.; Gao, G. F.; Wu, G.; Chen, W.; Shi, W.; Tan, W. Genomic characterisation and epidemiology of 2019 novel coronavirus: implications for virus origins and receptor binding. *Lancet* **2020**, *395* (10224), 565−574.

(3) Malone, B.; Urakova, N.; Snijder, E. J.; Campbell, E. A. Structures and functions of coronavirus replication-transcription complexes and their relevance for SARS-CoV-2 drug design. *Nature reviews. Molecular cell biology* **2022**, *23* (1), 21−39.

(4) Bai, Z.; Cao, Y.; Liu, W.; Li, J. The SARS-CoV-2 Nucleocapsid Protein and Its Role in Viral Structure, Biological Functions, and a Potential Target for Drug or Vaccine Mitigation. *Viruses* **2021**, *13* (6), 1115.

(5) Goodsell, D. S.; Dutta, S.; Zardecki, C.; Voigt, M.; Berman, H. M.; Burley, S. K. The RCSB PDB "Molecule of the Month": Inspiring a Molecular View of Biology. *PLoS Biol.* **2015**, *13* (5), No. e1002140.

(6) Cao, L.; Goreshnik, I.; Coventry, B.; Case, J. B.; Miller, L.; Kozodoy, L.; Chen, R. E.; Carter, L.; Walls, A. C.; Park, Y. J.; Strauch, E. M.; Stewart, L.; Diamond, M. S.; Veesler, D.; Baker, D. De novo design of picomolar SARS-CoV-2 miniprotein inhibitors. *Science* **2020**, *370* (6515), 426−431.

(7) Tsai, M. S.; Shih, W. T.; Yang, Y. H.; Lin, Y. S.; Chang, G. H.; Hsu, C. M.; Yeh, R. A.; Shu, L. H.; Cheng, Y. C.; Liu, H. T.; et al. Potential inhibitor for blocking binding between ACE2 and SARS-CoV-2 spike protein with mutations. *Biomedecine Pharmacotherapie* **2022**, *149*, No. 112802.

(8) Thijssen, V.; Hurdiss, D. L.; Debski-Antoniak, O. J.; Spence, M. A.; Franck, C.; Norman, A.; Aggarwal, A.; Mokiem, N. J.; van Dongen, D. A. A.; Vermeir, S. W.; et al. A broad-spectrum macrocyclic peptide inhibitor of the SARS-CoV-2 spike protein. *Proc. Natl. Acad. Sci. U.S.A.* **2023**, *120* (26), No. e2303292120.

(9) Li, C.; Zhou, H.; Guo, L.; Xie, D.; He, H.; Zhang, H.; Liu, Y.; Peng, L.; Zheng, L.; Lu, W.; et al. Potential inhibitors for blocking the interaction of the coronavirus SARS-CoV-2 spike protein and its host cell receptor ACE2. *Journal of translational medicine* **2022**, *20* (1), 314.

(10) Wu, J.; Zhang, J.; Zhang, H. X. Computational Design of Miniprotein Inhibitors Targeting SARS-CoV-2 Spike Protein. *Langmuir: the ACS journal of surfaces and colloids* **2022**, *38* (34), 10690−10703.

(11) Valiente, P. A.; Wen, H.; Nim, S.; Lee, J.; Kim, H. J.; Kim, J.; Perez-Riba, A.; Paudel, Y. P.; Hwang, I.; Kim, K. D.; Kim, S.; Kim, P. M. Computational Design of Potent D-Peptide Inhibitors of SARS-CoV-2. *J. Med. Chem.* **2021**, *64*, 14955−14967.

(12) Li, Q.; Wu, J.; Nie, J.; Zhang, L.; Hao, H.; Liu, S.; Zhao, C.; Zhang, Q.; Liu, H.; Nie, L.; et al. The Impact of Mutations in SARS-CoV-2 Spike on Viral Infectivity and Antigenicity. *Cell* **2020**, *182* (5), 1284.

(13) Sharma, P. L.; Nurpeisov, V.; Hernandez-Santiago, B.; Beltran, T.; Schinazi, R. F. Nucleoside inhibitors of human immunodeficiency virus type 1 reverse transcriptase. *Current topics in medicinal chemistry* **2004**, *4* (9), 895−919.

(14) Tian, L.; Qiang, T.; Liang, C.; Ren, X.; Jia, M.; Zhang, J.; Li, J.; Wan, M.; YuWen, X.; Li, H.; Cao, W.; Liu, H. RNA-dependent RNA polymerase (RdRp) inhibitors: The current landscape and repurposing for the COVID-19 pandemic. *European journal of medicinal chemistry* **2021**, *213*, No. 113201.

(15) Wang, M.; Cao, R.; Zhang, L.; Yang, X.; Liu, J.; Xu, M.; Shi, Z.; Hu, Z.; Zhong, W.; Xiao, G. Remdesivir and chloroquine effectively inhibit the recently emerged novel coronavirus (2019-nCoV) in vitro. *Cell research* **2020**, *30* (3), 269−271.

(16) Tong, S.; Su, Y.; Yu, Y.; Wu, C.; Chen, J.; Wang, S.; Jiang, J. Ribavirin therapy for severe COVID-19: a retrospective cohort study. *International journal of antimicrobial agents* **2020**, *56* (3), No. 106114.

(17) Beigel, J. H.; Nam, H. H.; Adams, P. L.; Krafft, A.; Ince, W. L.; El-Kamary, S. S.; Sims, A. C. Advances in respiratory virus therapeutics - A meeting report from the 6th isirv Antiviral Group conference. *Antiviral research* **2019**, *167*, 45−67.

(18) He, Y.; Zhou, Y.; Wu, H.; Kou, Z.; Liu, S.; Jiang, S. Mapping of antigenic sites on the nucleocapsid protein of the severe acute respiratory syndrome coronavirus. *Journal of clinical microbiology* **2004**, *42* (11), 5309−14.
(19) Masters, P. S.; Sturman, L. S. Background paper. Functions of the coronavirus nucleocapsid protein. *Advances in experimental medicine and biology* **1990**, *276*, 235−8.
(20) Lin, S. M.; Lin, S. C.; Hsu, J. N.; Chang, C. K.; Chien, C. M.; Wang, Y. S.; Wu, H. Y.; Jeng, U. S.; Kehn-Hall, K.; Hou, M. H. Structure-Based Stabilization of Non-native Protein-Protein Interactions of Coronavirus Nucleocapsid Proteins in Antiviral Drug Design. *Journal of medicinal chemistry* **2020**, *63* (6), 3131−3141.
(21) Dai, W.; Zhang, B.; Jiang, X. M.; Su, H.; Li, J.; Zhao, Y.; Xie, X.; Jin, Z.; Peng, J.; Liu, F.; Li, C.; Li, Y.; Bai, F.; Wang, H.; Cheng, X.; Cen, X.; Hu, S.; Yang, X.; Wang, J.; Liu, X.; Xiao, G.; Jiang, H.; Rao, Z.; Zhang, L. K.; Xu, Y.; Yang, H.; Liu, H. Structure-based design of antiviral drug candidates targeting the SARS-CoV-2 main protease. *Science* **2020**, *368* (6497), 1331−1335.
(22) Silva, R. C.; Freitas, H. F.; Campos, J. M.; Kimani, N. M.; Silva, C.; Borges, R. S.; Pita, S. S. R.; Santos, C. B. R. Natural Products-Based Drug Design against SARS-CoV-2 Mpro 3CLpro. *International journal of molecular sciences* **2021**, *22* (21), 11739.
(23) Elend, L.; Jacobsen, L.; Cofala, T.; Prellberg, J.; Teusch, T.; Kramer, O.; Solov'yov, I. A. Design of SARS-CoV-2 Main Protease Inhibitors Using Artificial Intelligence and Molecular Dynamic Simulations. *Molecules* **2022**, *27* (13), 4020.
(24) Stefanelli, I.; Corona, A.; Cerchia, C.; Cassese, E.; Improta, S.; Costanzi, E.; Pelliccia, S.; Morasso, S.; Esposito, F.; Paulis, A.; Scognamiglio, S.; Di Leva, F. S.; Storici, P.; Brindisi, M.; Tramontano, E.; Cannalire, R.; Summa, V. Broad-spectrum coronavirus 3C-like protease peptidomimetic inhibitors effectively block SARS-CoV-2 replication in cells: Design, synthesis, biological evaluation, and X-ray structure determination. *Eur. J. Med. Chem.* **2023**, *253*, No. 115311.
(25) Elagawany, M.; Elmaaty, A. A.; Mostafa, A.; Abo Shama, N. M.; Santali, E. Y.; Elgendy, B.; Al-Karmalawy, A. A. Ligand-based design, synthesis, computational insights, and in vitro studies of novel N-(5-Nitrothiazol-2-yl)-carboxamido derivatives as potent inhibitors of SARS-CoV-2 main protease. *J. Enzyme Inhib Med. Chem.* **2022**, *37*, 2112−2132.
(26) Westberg, M.; Su, Y.; Zou, X.; Huang, P.; Rustagi, A.; Garhyan, J.; Patel, P. B.; Fernandez, D.; Wu, Y.; Hao, C.; et al. An orally bioavailable SARS-CoV-2 main protease inhibitor exhibits improved affinity and reduced sensitivity to mutations. *Sci. Transl Med.* **2024**, *16*, No. eadi0979.
(27) Jiang, X.; Su, H.; Shang, W.; Zhou, F.; Zhang, Y.; Zhao, W.; Zhang, Q.; Xie, H.; Jiang, L.; Nie, T.; et al. Structure-based development and preclinical evaluation of the SARS-CoV-2 3C-like protease inhibitor simnotrelvir. *Nat. Commun.* **2023**, *14*, 6463.
(28) Zhang, S.; Krumberger, M.; Morris, M. A.; Parrocha, C. M. T.; Kreutzer, A. G.; Nowick, J. S. Structure-based drug design of an inhibitor of the SARS-CoV-2 (COVID-19) main protease using free software: A tutorial for students and scientists. *Eur. J. Med. Chem.* **2021**, *218*, No. 113390.
(29) Joshi, R. P.; Schultz, K. J.; Wilson, J. W.; Kruel, A.; Varikoti, R. A.; Kombala, C. J.; Kneller, D. W.; Galanie, S.; Phillips, G.; Zhang, Q.; Coates, L.; Parvathareddy, J.; Surendranathan, S.; Kong, Y.; Clyde, A.; Ramanathan, A.; Jonsson, C. B.; Brandvold, K. R.; Zhou, M.; Head, M. S.; Kovalevsky, A.; Kumar, N. AI-Accelerated Design of Targeted Covalent Inhibitors for SARS-CoV-2. *J. Chem. Inf Model* **2023**, *63*, 1438−1453.
(30) Hassan, H.; Chiavaralli, J.; Hassan, A.; Bedda, L.; Krischuns, T.; Chen, K. Y.; Li, A. S. M.; Delpal, A.; Decroly, E.; Vedadi, M.; Naffakh, N.; Agou, F.; Mallart, S.; Arafa, R. K.; Arimondo, P. B. Design and synthesis of naturally-inspired SARS-CoV-2 inhibitors. *RSC Med. Chem.* **2023**, *14*, 507−519.
(31) Egli, M.; Manoharan, M. Chemistry, structure and function of approved oligonucleotide therapeutics. *Nucleic acids research* **2023**, *51* (6), 2529−2573.
(32) Dowdy, S. F.; Setten, R. L.; Cui, X. S.; Jadhav, S. G. Delivery of RNA Therapeutics: The Great Endosomal Escape! *Nucleic acid therapeutics* **2022**, *32* (5), 361−368.
(33) Quemener, A. M.; Galibert, M. D. Antisense oligonucleotide: A promising therapeutic option to beat COVID-19. *Wiley interdisciplinary reviews. RNA* **2022**, *13* (4), No. e1703.
(34) Neuman, B. W.; Stein, D. A.; Kroeker, A. D.; Paulino, A. D.; Moulton, H. M.; Iversen, P. L.; Buchmeier, M. J. Antisense morpholino-oligomers directed against the 5′ end of the genome inhibit coronavirus proliferation and growth. *Journal of virology* **2004**, *78* (11), 5891−9.
(35) Sun, L.; Li, P.; Ju, X.; Rao, J.; Huang, W.; Ren, L.; Zhang, S.; Xiong, T.; Xu, K.; Zhou, X.; et al. In vivo structural characterization of the SARS-CoV-2 RNA genome identifies host proteins vulnerable to repurposed drugs. *Cell* **2021**, *184* (7), 1865−1883.
(36) Manfredonia, I.; Nithin, C.; Ponce-Salvatierra, A.; Ghosh, P.; Wirecki, T. K.; Marinus, T.; Ogando, N. S.; Snijder, E. J.; van Hemert, M. J.; Bujnicki, J. M.; Incarnato, D. Genome-wide mapping of SARS-CoV-2 RNA structures identifies therapeutically-relevant elements. *Nucleic acids research* **2020**, *48* (22), 12436−12452.
(37) Huston, N. C.; Wan, H.; Strine, M. S.; de Cesaris Araujo Tavares, R.; Wilen, C. B.; Pyle, A. M. Comprehensive in vivo secondary structure of the SARS-CoV-2 genome reveals novel regulatory motifs and mechanisms. *Molecular cell* **2021**, *81* (3), 584−598.
(38) V'Kovski, P.; Kratzel, A.; Steiner, S.; Stalder, H.; Thiel, V. Coronavirus biology and replication: implications for SARS-CoV-2. *Nature reviews. Microbiology* **2021**, *19* (3), 155−170.
(39) Rangan, R.; Zheludev, I. N.; Hagey, R. J.; Pham, E. A.; Wayment-Steele, H. K.; Glenn, J. S.; Das, R. RNA genome conservation and secondary structure in SARS-CoV-2 and SARS-related viruses: a first look. *Rna* **2020**, *26* (8), 937−959.
(40) Gumna, J.; Antczak, M.; Adamiak, R. W.; Bujnicki, J. M.; Chen, S. J.; Ding, F.; Ghosh, P.; Li, J.; Mukherjee, S.; Nithin, C.; Pachulska-Wieczorek, K.; Ponce-Salvatierra, A.; Popenda, M.; Sarzynska, J.; Wirecki, T.; Zhang, D.; Zhang, S.; Zok, T.; Westhof, E.; Miao, Z.; Szachniuk, M.; Rybarczyk, A. Computational Pipeline for Reference-Free Comparative Analysis of RNA 3D Structures Applied to SARS-CoV-2 UTR Models. *Int. J. Mol. Sci.* **2022**, *23* (17), 9630.
(41) Lorenz, R.; Bernhart, S. H.; Honer Zu Siederdissen, C.; Tafer, H.; Flamm, C.; Stadler, P. F.; Hofacker, I. L. ViennaRNA Package 2.0. *Algorithms for molecular biology: AMB* **2011**, *6*, 26.
(42) Sarzynska, J.; Popenda, M.; Antczak, M.; Szachniuk, M. RNA tertiary structure prediction using RNAComposer in CASP15. *Proteins* **2023**, *91* (12), 1790−1799.
(43) Popenda, M.; Szachniuk, M.; Antczak, M.; Purzycka, K. J.; Lukasiak, P.; Bartol, N.; Blazewicz, J.; Adamiak, R. W. Automated 3D structure composition for large RNAs. *Nucleic acids research* **2012**, *40* (14), No. e112.
(44) Mansoor, M.; Melendez, A. J. Advances in antisense oligonucleotide development for target identification, validation, and as novel therapeutics. *Gene regulation and systems biology* **2008**, *2*, GRSB.S418.
(45) Crooke, S. T.; Witztum, J. L.; Bennett, C. F.; Baker, B. F. RNA-Targeted Therapeutics. *Cell metabolism* **2018**, *27* (4), 714−739.
(46) Ottesen, E. W. ISS-N1 makes the First FDA-approved Drug for Spinal Muscular Atrophy. *Translational neuroscience* **2017**, *8*, 1−6.
(47) Shiraishi, T.; Eysturskarð, J.; Nielsen, P. E Modulation of mdm2 pre-mRNA splicing by 9-aminoacridine-PNA (peptide nucleic acid) conjugates targeting intron-exon junctions. *BMC cancer* **2010**, *10*, 342.
(48) Watts, K. S.; Dalal, P.; Tebben, A. J.; Cheney, D. L.; Shelley, J. C. Macrocycle conformational sampling with MacroModel. *J. Chem. Inf. Model.* **2014**, *54* (10), 2680−96.
(49) He, J.; Wang, J.; Tao, H.; Xiao, Y.; Huang, S. Y. HNADOCK: a nucleic acid docking server for modeling RNA/DNA-RNA/DNA 3D complex structures. *Nucleic acids research* **2019**, *47* (W1), W35−W42.

https://doi.org/10.1021/acsomega.4c04023
ACS Omega 2024, 9, 33000−33010

(50) Repasky, M. P.; Shelley, M.; Friesner, R. A. Flexible Ligand Docking with Glide. In *Current Protocols in Bioinformatics*; Wiley, 2007; Chapter 8, Unit 8 12. DOI: 10.1002/0471250953.bi0812s18
(51) Macfarlane, L. A.; Murphy, P. R. MicroRNA: Biogenesis, Function and Role in Cancer. *Current genomics* **2010**, *11* (7), 537−61.
(52) Iwakawa, H. O.; Tomari, Y. Life of RISC: Formation, action, and degradation of RNA-induced silencing complex. *Molecular cell* **2022**, *82* (1), 30−43.
(53) Halgren, T. A. Identifying and characterizing binding sites and assessing druggability. *J. Chem. Inf. Model.* **2009**, *49* (2), 377−89.
(54) Madhavi Sastry, G.; Adzhigirey, M.; Day, T.; Annabhimoju, R.; Sherman, W. Protein and ligand preparation: parameters, protocols, and influence on virtual screening enrichments. *Journal of computer-aided molecular design* **2013**, *27* (3), 221−234.
(55) Grigoreva, T. A.; Vorona, S. V.; Novikova, D. S.; Tribulovich, V. G. Analysis of P-Glycoprotein Transport Cycle Reveals a New Way to Identify Efflux Inhibitors. *ACS omega* **2022**, *7* (47), 42835−42844.
(56) Novikova, D. S.; Grigoreva, T. A.; Ivanov, G. S.; Melino, G.; Barlev, N. A.; Tribulovich, V. G. Activating Effect of 3-Benzylidene Oxindoles on AMPK: From Computer Simulation to High-Content Screening. *ChemMedChem.* **2020**, *15* (24), 2521−2529.
(57) Bowers, K. J.; Chow, E.; Xu, H.; Dror, R. O.; Eastwood, M. P.; Gregersen, B. A.; Klepeis, J. L.; Kolossvary, I.; Moraes, M. A.; Sacerdoti, F. D.; Salmon, J. K.; Shan, Y.; Shaw, D. E., Scalable algorithms for molecular dynamics simulations on commodity clusters. *Proceedings of the 2006 ACM/IEEE Conference on Supercomputing*; Association for Computing Machinery: Tampa, FL, 2006.
(58) Desta, I. T.; Porter, K. A.; Xia, B.; Kozakov, D.; Vajda, S. Performance and Its Limits in Rigid Body Protein-Protein Docking. *Structure* **2020**, *28* (9), 1071−1081.

https://doi.org/10.1021/acsomega.4c04023
ACS Omega 2024, 9, 33000−33010